Modulational instability dynamics in a spatial focusing and temporal defocusing medium

D. Anderson, M. Karlsson, and M. Lisak
Institute for Electromagnetic Field Theory, Chalmers University of Technology, S-412 96 Göteborg, Sweden

A. Sergeev
Institute for Applied Physics, Nizhny Novgorod, Russia
(Received 1 October 1992)

The modulational instability of a wave in media where the nonlinearity has a focusing-in-space and defocusing-in-time character is investigated. An approximate self-similar solution of the nonlinear Schrödinger equation is derived for this nonlinearity and is used as background envelope of the wave. We show that this background wave envelope can initially enhance exponential growth of a transverse spatial modulation. The analysis is extended to the case of a modulation in both time and space, and it is found that such a spatiotemporal modulation can be unstable as well.

PACS number(s): 52.35.−g, 42.65.−k

I. INTRODUCTION

As is well known, the nonlinear Schrödinger (NLS) equation describing the evolution of a wave-field envelope represents a universal model for nonlinear wave propagation in many physical media, cf. [1–3]. This equation is

$$-i\frac{\partial E}{\partial z}+a\frac{\partial^2 E}{\partial t^2}+b\Delta_\perp E+E|E|^2=0\ , \tag{1}$$

where E is the wave envelope, t is the retarded time, x,y,z are normalized space coordinates, $\Delta_\perp=\partial^2/\partial x^2+\partial^2/\partial y^2$, and a and b are real constants. The signs of the coefficients a and b are determined by the group-velocity dispersion and the wave-vector surface curvature in k space, respectively. For $a,b>0$, Eq. (1) describes, depending on the field dimensionality, such extensively studied phenomena in nonlinear physics as solitary waves, self-focusing, collapse, etc. In the case of opposite signs of a and b, e.g., $a=-1$, $b=1$, Eq. (1) [here called the modified nonlinear Schrödinger (MNLS) equation] has been less studied in the literature in spite of the fact that it provides a proper model for describing the nonlinear dynamics of a wide class of waves, e.g., deep-water gravitational waves [4], lower-hybrid waves [5], cyclotron [6] waves in a magnetized plasma, and optical waves in media with positive (normal) group-velocity dispersion [7,8].

It turns out that, contrary to the classical NLS equation, the MNLS equation does not possess any localized stationary solutions, and the nonlinear dynamics in the frame of the MNLS equation may lead to wave collapse of a non-self-similar fractal character [9]. Considering a wave packet localized in time and (x,y) space, it can be shown, using the known integrals of Eq. (1) with $a=-1$ and $b=1$, that the following important relation is satisfied, cf. [9]:

$$\frac{\partial^2}{\partial z^2}\int t^2|E|^2dt\,dx\,dy=8\int\left[\left|\frac{\partial E}{\partial t}\right|^2+\frac{|E|^4}{4}\right]dt\,dx\,dy>0\ , \tag{2}$$

which states that the mean-square width of the wave packet is a monotonically increasing function of z. This implies that any structural modulation of the wave packet develops on a background field distribution that expands in time.

Since the nonlinearity in the MNLS equation is of a focusing-in-space and defocusing-in-time character, one would expect that the interplay between diffractive and dispersive effects, as well as the field distribution of the expanding background, should be important for the development of modulational instabilities. The case of modulation instability developing on a constant nonexpanding background was recently investigated [10], and it was found that spatiotemporal modulations could grow faster than pure spatial modes. Allowing the background to expand does, however, change the situation significantly. Different possibilities are conceivable. (i) The expansion of the background may suppress the transverse modulational instability and may result in self-focusing and/or collapse of the wave packet. (ii) The wave packet may be unstable in the time domain in spite of the nonlinear defocusing in time. (iii) In cases of unstable perturbations, what are the properties of the fastest growing mode?

The aim of the present paper is to explore these issues by investigating modulational instabilities on an expanding background within the framework of the MNLS equation. In Sec. II we will derive a suitable background distribution to the MNLS equation, and in Sec. III we investigate its sensitivity to transverse periodic perturbations in space. Finally, in Sec. IV the analysis is extended to include time-dependent perturbations as well.

II. MODEL FOR THE EXPANDING BACKGROUND

The main features of the modulation instability can be studied by assuming the background field distribution to be one dimensional ($\Delta_\perp=0$). Then the envelope of the background field E_b is described by the NLS equation

$$-i\frac{\partial E_b}{\partial z}-\frac{\partial^2 E_b}{\partial t^2}+|E_b|^2E_b=0\ , \tag{3}$$

separating E_b into real amplitude A and phase ϕ according to $E_b=A\exp(i\phi)$, we obtain from Eq. (3)

$$\frac{\partial}{\partial z}(A^2)+2\frac{\partial}{\partial t}(A^2\Omega)=0\ , \tag{4}$$

$$\frac{\partial\Omega}{\partial z}+\frac{\partial}{\partial t}(\Omega^2)=\frac{\partial}{\partial t}\left[\frac{1}{A}\frac{\partial^2 A}{\partial t^2}-A^2\right]\ , \tag{5}$$

where the chirp function Ω is defined by $\Omega=\partial\phi/\partial t$. We now assume that the term $(\partial^2A/\partial t^2)/A$ is small in comparison to A^2, which will be verified *a posteriori*. Thus, Eq. (5) can be approximated as

$$\frac{\partial\Omega}{\partial z}+\frac{\partial}{\partial t}(\Omega^2)=-\frac{\partial A^2}{\partial t}\ . \tag{6}$$

Looking for simple solutions to Eqs. (4) and (6), e.g., polynomial dependence of t, we realize by inspection that Eq. (4) implies Ω to be a first-degree polynomial in t. This is consistent with the two first terms of Eq. (6), and it also follows that A^2 is a second-degree polynomial in t, i.e., the pulse shape is parabolic. Thus, we can find self-similar solutions of the form $f(z)g[t/\tau(z)]$ for A and Ω, and we make the ansatz

$$A^2(z,t)=I(z)\left[1-\frac{t^2}{\tau(z)^2}\right]\ , \tag{7}$$

$$\Omega(z,t)=\alpha(z)t\ . \tag{8}$$

If we now compare the terms on the right-hand side of Eq. (5) we find that

$$\frac{A^2}{\left|\frac{1}{A}\frac{\partial^2A}{\partial t^2}\right|}=I\tau^2\left[1-\frac{t^2}{\tau^2}\right]^3\ . \tag{9}$$

This implies that for a high intensity pulse with $I\tau^2\gg1$, the term $(\partial^2A/\partial t^2)/A$ is small in a large part of the pulse and can be neglected, except very close to the pulse edges. Thus, for a strongly nonlinear pulse the analysis is consistent. Substituting the expressions (7) and (8) into Eqs. (4) and (6) and identifying powers of t we obtain the following equations for $I(z)$, $\tau(z)$, and $\alpha(z)$:

$$I(z)\tau(z)=I(0)\tau(0)=W=\text{const}\ , \tag{10}$$

$$\alpha^2(z)=2\frac{I^2(z)}{W^2}[I(0)-I(z)]\ , \tag{11}$$

$$\frac{\partial I}{\partial z}=-2\frac{I(z)^2}{W}\sqrt{2[I(0)-I(z)]}\ . \tag{12}$$

The implicit solution of Eq. (12) is

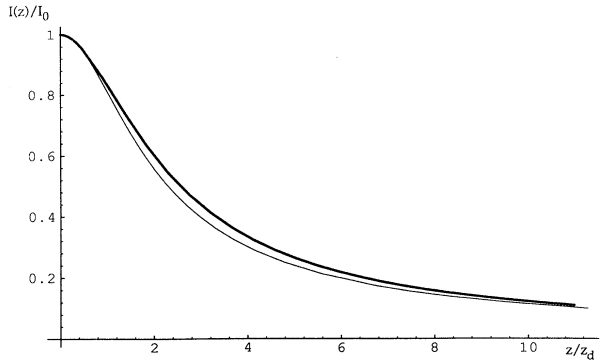

FIG. 1. Falloff in central intensity along the normalized distance of propagation. The thin line is the (exact) implicit relation given by Eq. (13), and the thick line is the approximate explicit relation of Eq. (15).

$$\frac{I(0)}{I(z)}\left[1-\frac{I(z)}{I(0)}\right]^{1/2}+\text{arctanh}\left[\left[1-\frac{I(z)}{I(0)}\right]^{1/2}\right]=[2I(0)]^{3/2}\frac{z}{W}\ . \tag{13}$$

Figures 1 and 2 show the variations of $I(z)$ and $\alpha(z)$, respectively, according to Eqs. (13) and (11). The intensity $I(z)$ is monotonically decreasing, and for large values of z it decays asymptotically as

$$I(z)\cong\frac{W}{2\sqrt{2I(0)}}\frac{1}{z}\equiv I(0)\frac{z_d}{z}\ . \tag{14}$$

A characteristic length of dispersion, z_d has been introduced as $W/[2I(0)]^{3/2}$ in the last expression. A good, empirical approximation to $I(z)$ is given by the function

$$I(z)\approx I(0)\frac{zz_d+4z_d^2}{z^2+zz_d+4z_d^2}\ , \tag{15}$$

which preserves the first and second derivative of $I(z)$ at $z=0$, as well as the asymptotic behavior for large z, see Fig. 1. According to Fig. 2, the chirp function $\alpha(z)$ first reaches a maximum value $\alpha_m=3^{-3/2}/z_d$, which is at-

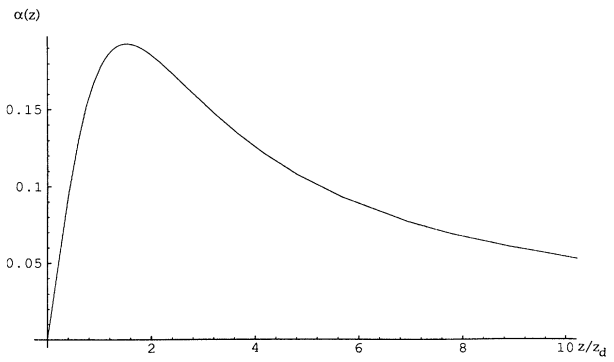

FIG. 2. The chirp function $\alpha(z)$ vs distance in the case $z_d=1$.

tained at the distance

$$z_m = z_d \left[\frac{\sqrt{3}}{2} - \frac{\pi}{6} \right] , \tag{16}$$

and then decays asymptotically as $\alpha(z) \approx 1/2z$ for large z ($z \gg z_m$). We also note from Eq. (10) that the width of the pulse $\tau(z)$ increases asymptotically for large z as

$$\tau(z) \cong 2\sqrt{2I(0)}z . \tag{17}$$

In summary, the envelope of the background pulse is given by

$$E_b(z,t) = \left\{ I(z) \left[1 - \left[\frac{t}{\tau(z)} \right]^2 \right]^{1/2} \right\} \times \exp \left[i \frac{\alpha(z) t^2}{2} + i \int I(z) dz \right] , \tag{18}$$

where the functions $I(z)$, $\alpha(z)$, and $\tau(z)$ are determined by Eqs. (10), (11), and (13).

III. TRANSVERSE SPATIAL PERTURBATIONS

We will start the perturbative analysis with the case of a time-independent perturbation of the background. The perturbed field is assumed to be of the form $E_b(z,t)[1+\epsilon(x,y,z)]$, where $|\epsilon| \ll 1$, and $E_b(z,t)$ is given by Eq. (18). This is inserted in Eq. (1) (with $a=-1$, $b=1$), and the resulting linearized equation becomes

$$i \frac{\partial \epsilon}{\partial z} = \Delta_\perp \epsilon - \frac{A_{tt}''}{A} + A^2(\epsilon + \epsilon^*) , \tag{19}$$

which is evaluated at $t=0$, i.e., the perturbation is for simplicity considered to be at the pulse center. Note that the small term A_{tt}''/A, which was neglected when the background was determined [cf. Eqs. (8) and (9)], is here assumed to be of the order $O(\epsilon)$ and has to be retained. Now, considering transverse periodical perturbations with wave number κ, we can write $\Delta_\perp \epsilon = -\kappa^2 \epsilon$, and defining $\epsilon = g(x,y,z) + if(x,y,z)$, the real and imaginary parts of Eq. (19) can be separated. Thus, the equations governing g and f will become

$$\frac{\partial^2 g}{\partial z^2} + \kappa^2[\kappa^2 - 2I(z)]g = \frac{I^2(z)}{2W^2}\kappa^2 , \tag{20a}$$

$$\kappa^2 f = -\frac{\partial g}{\partial z} , \tag{20b}$$

where the term on the rhs in Eq. (20a) arises from A_{tt}''/A evaluated at $t=0$. We neglect this term to start with, and concentrate on the homogeneous equation for g. Exponential growth can occur if $2I(z) > \kappa^2$, similar to the case of conventional modulational instability. This implies that the gain a perturbation exhibits (corresponding to a certain value of κ) will change along the distance of propagation, see Fig. 3. At the distance $z > z_0$, where z_0 is defined by $2I(z_0) = \kappa^2$, the quantity in the brackets of Eq. (20a) becomes positive, and g becomes oscillatory. Since $I(z)$ decreases as z^{-1} at large distances, the behavior of g will in this limit be that of a Coulomb wave

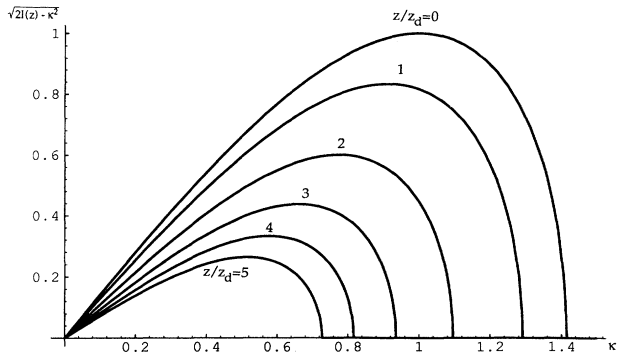

FIG. 3. Gain spectra of the modulation instability at different distances of propagation. We have used $I_0=1$ and considered $z/z_d = 0,1,2,3,4,5$.

function [11], and the amplitude of the oscillations will be of the order $g(z_0)$. Note that the perturbation after the growth stage will not be damped out, but will oscillate with the period κ^2 in the long-distance limit. Consequently, a transverse periodic perturbation of the period κ will develop into a longitudinal oscillation of the period κ^2, thus manifesting a form of "frequency squaring."

All these features are apparent in the numerical solutions of Eq. (20a), shown in Fig. 4. In these simulations we have examined the normalized perturbation $g(z)/g(0)$, where we have assumed $g'(0)=0$. In Fig. 4(a) the homogeneous part of the solution of Eq. (20a) is plotted with a few different values of κ. Note that the strongest perturbations at long distances have a small value of κ, whereas at small distances the larger values of κ dominate, cf. Fig. 3. The influence of different strengths of the rhs term in Eq. (20a) can be seen in Fig. 4(b). This term does not affect the qualitative behavior of the homogeneous solution, but it increases the maximum values of g. For larger values of z (past the first maximum of g) the solution appears to be the homogeneous, multiplied with some constant factor. Thus, in order to examine the qualitative behavior of g, it suffices to examine the homogeneous equation.

Exact analytical solutions to the homogeneous Eq. (20a) are not available, but a quantitative approximation of g can be found using the WKB approximation [12]. In this approach, the second derivative $g''(z)$ is assumed to be small, and g can be approximated with $g \sim \exp[\Gamma(z)]$, where

$$\Gamma(z) = \int_0^z \kappa[2I(z') - \kappa^2]^{1/2} dz' . \tag{21}$$

Specifically, the value $g(z_0)$ can be calculated from this integral by changing the variable of integration from z to I by using Eq. (12), and thus

$$g(z_0) \approx \exp \left[\frac{\pi W(2I_0 - \kappa^2)}{2(2I_0)^{3/2}} \right] = \exp \left[\frac{\pi z_d}{2}(2I_0 - \kappa^2) \right] . \tag{22}$$

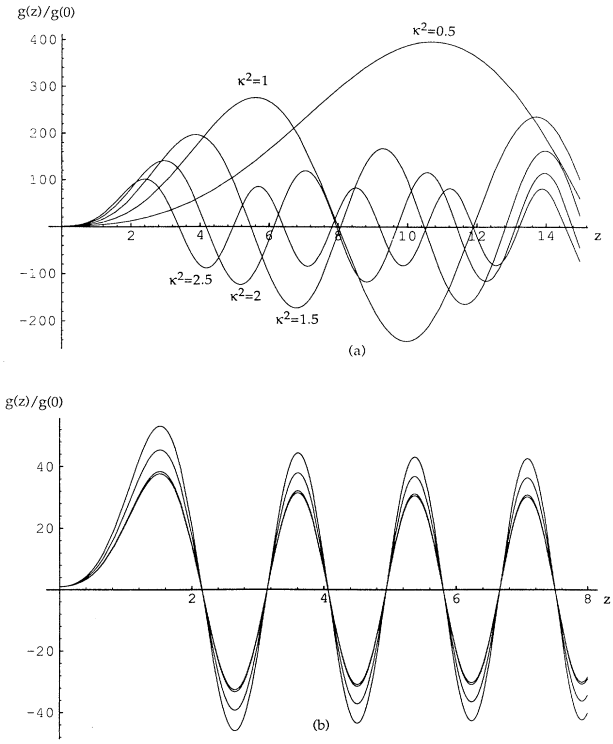

FIG. 4. (a) Homogeneous solution of Eq. (20a). Note that we plot the normalized perturbation $g(z)/g(0)$. Equation (15) has been used for $I(z)$, along with $I_0=5$, $W=10$, and κ^2, taking the values 0.5,1,1.5,2,2.5. The lower values of κ have higher amplitudes and longer distances to the first maximum. (b) Full solution to Eq. (20a), including the rhs term $[I(z)\kappa/W]^2/[2g(0)]$ for the same values as in (a) but with $\kappa^2=4$. The curve with lowest amplitude is the homogeneous solution, and the other three curves correspond to (in growing order) $g(0)=1,0.1,0.05$.

This relation shows that the growth of a perturbation of wave number κ up to the distance z_0 will be larger the less κ is. The lower gain for small values of κ is compensated by a longer distance of growth z_0. Therefore, if we consider distances long enough the lowest wave numbers κ will dominate. If this is *not* the fact, i.e., if some arbitrary distance is considered, the natural question arises: Given a certain distance of propagation z_1 and initial intensity I_0, which κ value will yield the strongest perturbation? The answer of this question requires the evaluation of the integral [Eq. (21)] at an arbitrary distance z_1. This gives us

$$\Gamma(z_1)=\frac{W}{\sqrt{2I_0}}\left\{(1-k^2)\arctan\left[k\left[\frac{1-\tilde{I}}{\tilde{I}-k^2}\right]^{1/2}\right]+\frac{k}{\tilde{I}}[(\tilde{I}-k^2)(1-\tilde{I})]^{1/2}\right\}=\frac{\pi W}{2\sqrt{2I_0}}\Phi(\tilde{I},k)\ , \tag{23}$$

where $k^2=\kappa^2/(2I_0)$ and $\tilde{I}=I(z_1)/I_0$. Here, the introduced function $\Phi(\tilde{I},k)$ is only defined in the regime $k^2<\tilde{I}<1$, or equivalently $0<z_1<z_0$. Note that $\Phi(\tilde{I},k)$ reduces to $1-k^2$ when $\tilde{I}=k^2$, or when $z_1=z_0$. The function $\Phi(\tilde{I},k)$ gives a measure of how strong a certain perturbation (corresponding to a certain value of k) is at a distance z_1 (corresponding to a certain value of $\tilde{I}$), and it is plotted in Fig. 5.

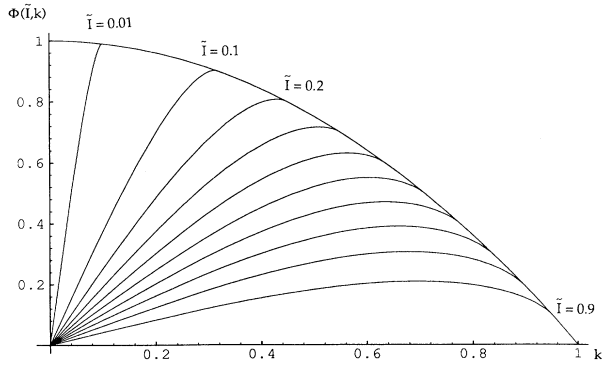

FIG. 5. Plot of the function $\Phi(I,k)$ showing the relative amplitudes of perturbations that have different values of k at different distances corresponding to the values of I.

IV. TEMPORAL PERTURBATIONS

Let us now consider a time-dependent perturbation. We will restrict the analysis to the asymptotic behavior at large z and consider the background pulse at $t=0$. Then the perturbed field has the form

$$E(z,t)=[1+\epsilon(z,t)]\left[I_0\frac{z_d}{z}\right]^{1/2}\exp\left[i\frac{t^2}{4z}-iI_0z_d\ln(z)\right]\ , \tag{24}$$

where z_d was defined in Sec. II. Substituting this into Eq. (1) we find to the first order in ϵ:

$$i\frac{\partial\epsilon}{\partial z}=\Delta_\perp\epsilon-\frac{\partial^2\epsilon}{\partial t^2}+i\frac{t}{z}\frac{\partial\epsilon}{\partial t}+I_0\frac{z_d}{z}(\epsilon+\epsilon^*)\ . \tag{25}$$

Comparing with the corresponding relation for a time-independent perturbation, Eq. (19), we find two additional terms arising from the time dependence of ϵ. We have also neglected the A''/A term, because it will not qualitatively affect the solutions, as discussed in the preceding chapter. In order to treat Eq. (25) we introduce new variables

$$z'=z\ ,\quad \zeta=\frac{t}{z}\ , \tag{26}$$

which transform Eq. (25) into

$$i\frac{\partial\epsilon}{\partial z'}=\Delta_\perp\epsilon-\frac{1}{z'^2}\frac{\partial^2\epsilon}{\partial\zeta^2}+I_0\frac{z_d}{z}(\epsilon+\epsilon^*)\ . \tag{27}$$

At this stage it is suitable to define the spatiotemporal wave numbers κ_ζ and $\kappa_\perp$ by

$$\frac{\partial^2\epsilon}{\partial\xi^2}\equiv-\kappa_\xi^2\epsilon\ ,\quad \Delta_\perp\epsilon\equiv-\kappa_\perp^2\epsilon\ . \tag{28}$$

Then separating Eq. (27) into the real and imaginary parts by taking $\epsilon=g+if$, we obtain the following equation for $g(z)$:

$$\frac{\partial^2 g}{\partial z^2}\frac{z^2}{(\kappa_\xi^2-\kappa_\perp^2 z^2)}+\frac{\partial g}{\partial z}\frac{2z\kappa_\xi^2}{(\kappa_\xi^2-\kappa_\perp^2 z^2)^2}+g\frac{(\kappa_\xi^2-\kappa_\perp^2 z^2)}{z^2}=-\frac{2I_0 z_d}{z}g\ , \tag{29}$$

where we have dropped the primes on the z coordinate. Equation (29) can be simplified by rescaling the z axis through

$$\xi=z+\alpha^2/z\ , \tag{30}$$

where $\alpha^2=(\kappa_\xi/\kappa_\perp)^2$. The resulting equation for $g(\xi)$ is then

$$\frac{\partial^2 g}{\partial\xi^2}+\kappa_\perp^2\left[\kappa_\perp^2-\frac{2I_0 z_d}{(\xi^2-4\alpha^2)^{1/2}}\right]g(\xi)=0\ . \tag{31}$$

Note that Eq. (31) reduces to Eq. (20a) in the limit $\alpha^2\to 0$, i.e., when the temporal perturbation vanishes. Equation (31) has been solved numerically in a few cases as illustrated in Figs. 6(a) and 6(b). The evolution of $g(x)$ is shown for different transverse spatial perturbations in Fig. 6(a), and for different modulation frequencies in time in Fig. 6(b). It can be seen that the qualitative behavior of g is similar to that of Sec. III, with an initial exponential growth and oscillations at larger distances. As before the oscillations do not decay at long distances, but remain strong during propagation. Note, however, that a different scaling is used on the z axis here. It follows from the transformation (30) that $\xi\geq 2\alpha$, where the equality corresponds to $z=\alpha$. For simplicity we will therefore restrict the analysis to values of z above α. This is also in agreement with the assumption of asymptotic behavior of the background, i.e., that z is above z_d. Thus, α has to be greater than z_d if this calculation is to be consistent.

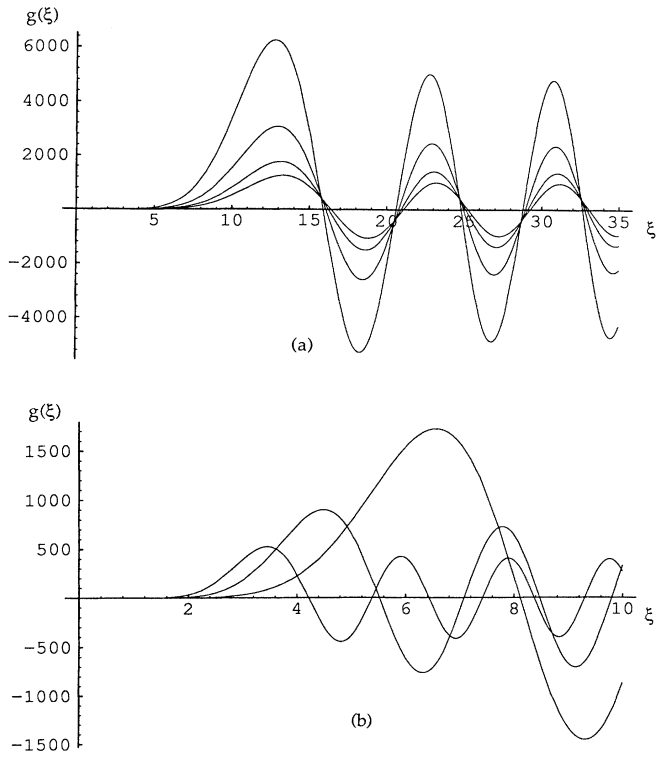

FIG. 6 (a). Evolution of a spatiotemporal perturbation on a background having $I_0=5$ and $z_d=1$. We have fixed the spatial modulation to $\kappa_\perp=1$ and the curves correspond to (in growing order) $\kappa_\xi^2=5,4,3,2$. (b) Same as (a), but for $\kappa_\xi^2=2$, and the curves correspond to (in growing order) $\kappa_\perp^2=4,3,2$.

The growth rate $\Gamma(\xi)$ of $g(\xi)$ at a specific value of ξ may, similar to the previous section, be WKB approximated with

$$\Gamma(\xi)=\kappa_\perp\int_{2\alpha}^{\xi}\left[\frac{2I_0 z_d}{(\xi^2-4\alpha^2)^{1/2}}-\kappa_\perp^2\right]^{1/2}d\xi\ . \tag{32}$$

The maximum growth rate $\Gamma_{\max}$ occurs when the upper limit is chosen as the value of ξ which makes the integrand vanish, i.e.,

$$\Gamma_{\max}=\Gamma\left[\xi=2\left[\alpha^2+\frac{I_0^2 z_d^2}{\kappa_\perp^4}\right]^{1/2}\right]=2I_0 z_d f(\delta)\ , \tag{33}$$

where

$$f(\delta)=\int_0^1\left[\frac{v(1-v)}{v^2+\delta^2}\right]^{1/2}dv\ ,\quad \delta=\frac{\kappa_\xi\kappa_\perp}{I_0 z_d}\ . \tag{34}$$

The function $f(\delta)$, plotted in Fig. 7, is monotonically decreasing with $f(0)=\pi/2$. As can be seen in Eq. (34), the wave numbers of the spatial and temporal modulations appear symmetrically, which implies that the maximum value of the perturbation is independent of whether the highest modulation frequency is in time or in space. We also note that, as in the case of pure spatial perturbations, $\Gamma_{\max}$ is larger the less the perturbation wave number is, and this is due to the longer distance of propagation be-

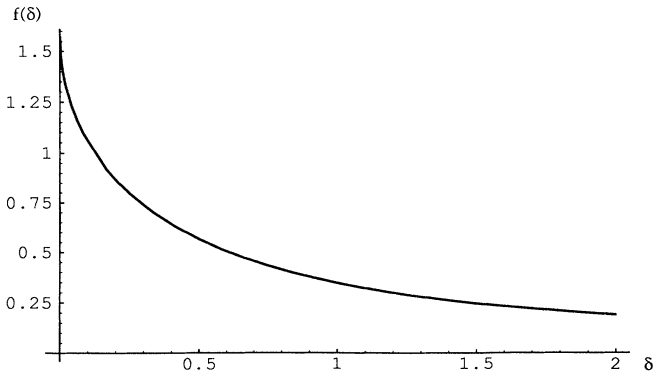

FIG. 7. Function $f(\delta)$ as defined by Eq. (34).

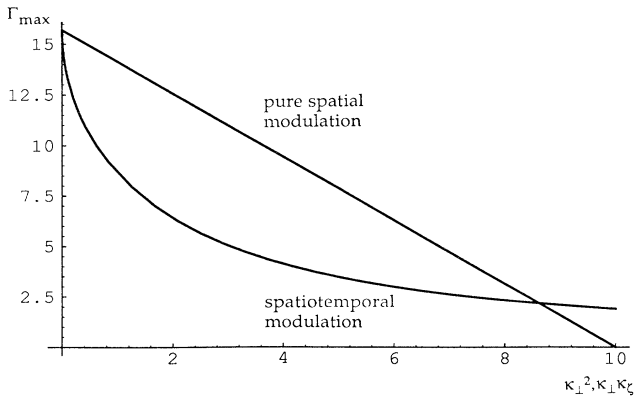

FIG. 8. Comparison of Γ_{max} vs $\kappa_\perp^2$ for the pure spatial modulation, and vs $\kappa_\perp \kappa_\zeta$ in the case of a spatiotemporal modulation. We have used a background having $I_0 = 5$ and $z_d = 1$, and Eqs. (22) and (33), respectively.

fore cutoff for these wave numbers.

The fact that a temporal perturbation can exhibit exponential growth may seem surprising for media of a defocusing-in-time character. It is, however, essential to note that a perturbation cannot be in time *only* in order to grow, but it is strongly dependent on the existence of a transverse spatial perturbation. The spatial perturbation can be said to boost the temporal one. This can also be seen in a direct comparison between Γ_{max} for both a pure spatial and a spatiotemporal perturbation on the same expanding background pulse, see Fig. 8. A pure spatial modulation will always give a higher value of Γ_{max} than a spatiotemporal modulation at the same modulation frequency. However, at a given value of $\kappa_\perp$ we can decrease κ_ζ sufficiently so that Γ_{max} becomes higher in the spatiotemporal case than in the pure spatial. Thus in theory, there are temporal perturbations that can be boosted so much by the spatial perturbations that the perturbation amplitude becomes higher for a spatiotemporal modulation than for a pure spatial modulation. Note however that the requirement $\kappa_\zeta > \kappa_\perp z_d$ due to the condition $\alpha > z_d$ puts restrictions on this possibility.

V. CONCLUSIONS

In summary, we have analyzed modulational instabilities developing on an expanding background wave envelope in a nonlinear media having a focusing-in-space and defocusing-in-time character. We have shown that exponential growth of a periodic spatial perturbation is possible in the initial high-amplitude stages of a pulse that defocuses in time, and that this exponential growth at longer distances develops into nondecaying oscillations. We have also found the qualitative properties of the strongest perturbation at a given distance of propagation. Finally, when the perturbative modulation is allowed to vary in both time and transverse space, the instability exhibits qualitatively the same behavior. However, the spatial perturbation amplifies the temporal one due to the interplay between the dispersive and diffractive effects.

ACKNOWLEDGMENT

This work was partly supported by the Swedish National Board for Industrial and Technical Development.

[1] V. E. Zakharov, Zh. Eksp. Teor. Fiz. **62**, 1745 (1972) [Sov. Phys. JETP **35**, 908 (1972)].
[2] H. Hasimoto and H. Ono, J. Phys. Soc. Jpn. **33**, 805 (1971).
[3] A. Hasegawa, *Plasma Instabilities and Nonlinear Effects* (Springer, Berlin, 1975).
[4] Y. C. Yuen and B. M. Lake, *Solitons in Action* (Academic, New York, 1986), Chap. 5.
[5] A. G. Litvak, A. M. Sergeev, and N. A. Zharova, Pis'ma Zh. Tekh. Fiz. **5**, 86 (1979) [Sov. Tech. Phys. Lett. **5**, 33 (1979)].
[6] J. R. Myra and C. H. Lin, Phys. Fluids **23**, 2258 (1980).
[7] A. Hasegawa and F. Tappert, Appl. Phys. Lett. **23**, 142 (1973); **23**, 171 (1973).
[8] P. Chernev and V. Petrov, Opt. Lett. **17**, 172 (1992).
[9] N. A. Zharova, A. G. Litvak, T. A. Petrova, A. M. Sergeev, and A. D. Yunakovskij, Pis'ma Zh. Eksp. Teor. Fiz. **44**, 12 (1986) [JETP Lett. **44**, 13 (1986)].
[10] L. W. Liou, X. D. Cao, C. J. McKinstrie, and G. P. Agrawal, Phys. Rev. A **46**, 4202 (1992).
[11] *Handbook of Mathematical Functions*, edited by M. Abramowitz and I. Stegun (Dover, New York, 1970), Chap. 14.
[12] C. M. Bender and S. A. Orzag, *Advanced Mathematical Methods for Scientists and Engineers* (McGraw-Hill, New York, 1978), Chap. 10.